RL-TR-93-57
Final Technical Report
May 1993

VELOCITY MATCHED MILLIMETERWAVE ELECTRO-OPTIC MODULATOR

California Institute of Technology

William B. Bridges and Finbar T. Sheehy

APPROVED FOR PUBLIC RELEASE; DISTRIBUTION UNLIMITED.

Rome Laboratory
Air Force Materiel Command
Griffiss Air Force Base, New York

This report has been reviewed by the Rome Laboratory Public Affairs Office (PA) and is releasable to the National Technical Information Service (NTIS). At NTIS it will be releasable to the general public, including foreign nations.

RL-TR-93-57 has been reviewed and is approved for publication.

APPROVED: [signature]

NORMAN P. BERNSTEIN
Project Engineer

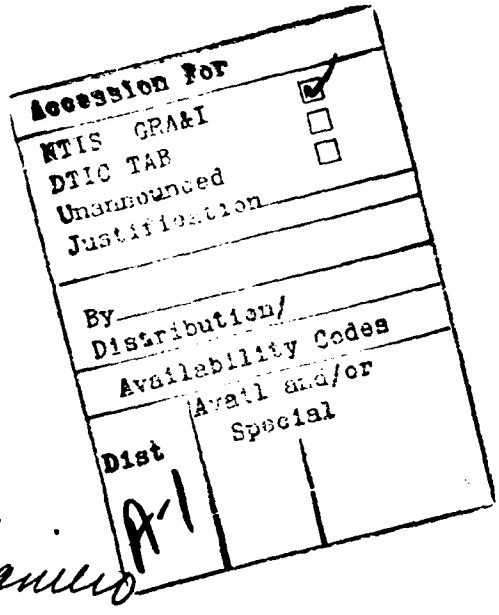

FOR THE COMMANDER: [signature]

JOHN A. GRANIERO
Chief Scientist
Command, Control & Communications Directorate

If your address has changed or if you wish to be removed from the Rome Laboratory mailing list, or if the addressee is no longer employed by your organization, please notify RL (C3DB) Griffiss AFB NY 13441. This will assist us in maintaining a current mailing list.

Do not return copies of this report unless contractual obligations or notices on a specific document require that it be returned.

REPORT DOCUMENTATION PAGE

Form Approved
OMB No. 0704-0188

1. AGENCY USE ONLY (Leave Blank)	2. REPORT DATE	3. REPORT TYPE AND DATES COVERED
	May 1993	Final Aug 90 - Sep 91

4. TITLE AND SUBTITLE
VELOCITY MATCHED MILLIMETERWAVE ELECTRO-OPTIC MODULATOR

5. FUNDING NUMBERS
C - F30602-88-D-0026,
Task 0021
PE - 63726F
PR - 2863
TA - 92
WU - PP

6. AUTHOR(S)
William B. Bridges and Finbar T. Sheehy

7. PERFORMING ORGANIZATION NAME(S) AND ADDRESS(ES)
California Institute of Technology
Dept of Electrical Engineering
ATTN: Dr. William Bridges
1201 E. California Blvd
Pasadena CA 91125

8. PERFORMING ORGANIZATION REPORT NUMBER
N/A

9. SPONSORING/MONITORING AGENCY NAME(S) AND ADDRESS(ES)
Rome Laboratory (C3DB)
525 Brooks Rd.
Griffiss AFB NY 13441-4505

10. SPONSORING/MONITORING AGENCY REPORT NUMBER
RL-TR-93-57

11. SUPPLEMENTARY NOTES
Rome Laboratory Project Engineer: Norman P. Bernstein/C3DB/(315) 330-7130

12a. DISTRIBUTION/AVAILABILITY STATEMENT
Approved for public release; distribution unlimited.

12b. DISTRIBUTION CODE

13. ABSTRACT (Maximum 200 words)

This effort has resulted in the fabrication and demonstration of an optical phase modulator at RF frequencies as high as 64 GHz while using a visible light source.

This technique, which is extendable to higher RF frequencies and to longer optical wavelengths, uses a series of high dielectric materials, set at an angle, between the RF signal source to match the resultant velocity of the RF wave with the optical signal in the photonic waveguide.

The coupling of the RF wave to the optical signal in the modulator is enhanced by plating resonant antenna structures onto the modulator substrate and electronically interfacing them with the modulator electrodes.

This technique can also be applied to interferometric type modulators.

14. SUBJECT TERMS	15. NUMBER OF PAGES
Modulators, Optical Modulators, Optical Devices, Microwave Millimeterwave	52
	16. PRICE CODE

17. SECURITY CLASSIFICATION OF REPORT	18. SECURITY CLASSIFICATION OF THIS PAGE	19. SECURITY CLASSIFICATION OF ABSTRACT	20. LIMITATION OF ABSTRACT
UNCLASSIFIED	UNCLASSIFIED	UNCLASSIFIED	UL

NSN 7540-01-280-5500

Standard Form 298 (Rev. 2-89)
Prescribed by ANSI Std. 239-18
298-102

I. EXECUTIVE SUMMARY

The phase velocity mismatch due to material dispersion in traveling-wave $LiNbO_3$ optical waveguide modulators may be greatly reduced by breaking the modulation transmission line into short segments and connecting each segment to its own surface antenna. The array of antennas is then illuminated by the modulation signal at an angle which produces a delay from antenna to antenna to match the optical waveguide's delay.

The program goal was to demonstrate experimentally the feasibility of antenna-coupled millimeter-wave electro-optic modulators. Initial experiments were to be performed at X-band, with mm-wave experiments to follow later.

We have:

- o Demonstrated antenna-coupled electro-optic phase modulators at 6-13 GHz and at 61 -64 GHz. Performance of these modulators was very promising [1,2].

- o Done theoretical work relating to modulator frequency response and performance, antennas and mm-wave feeds.

- o Examined possible configurations and established which ones are most promising.

II. INTRODUCTION

Electro-optic modulators using $LiNbO_3$ have been demonstrated with modulation frequencies over 17 GHz and with modulation voltages less than 1 V [3,4]. Unfortunately there is a trade-off between sensitivity and bandwidth. While $LiNbO_3$ has a high electro-optic coefficient, it is also dispersive, having a much higher refractive index for microwave frequencies than for optical signals. The consequent mismatch of optical and microwave phase velocities limits the useful interaction length to about one-quarter free-space wavelength at the microwave frequency. If the modulator is long, for high sensitivity, then the maximum modulation frequency is low: if the modulation frequency is high then the modulator must be kept short, limiting sensitivity. We have demonstrated a new technique which overcomes this limitation and, as an added benefit, uses a waveguide to introduce the modulation signal. This latter feature may prove as important as the former for modulators operating in the millimeter wave range.

There have been previous approaches to overcoming the material dispersion limitation to achieve high modulation frequencies. Alferness et al. [5] have demonstrated a technique in which the modulation electrodes are divided into sections, each of which introduces a phase error of 180° between the optical and modulating signals. The sections are then connected together with transpositions which correct the phase by 180°. In this way the average phase velocities of the two signals are kept equal. Some loss of sensitivity does occur because the electrode length which is required to introduce the 180° phase error is quite long.

Schaffner [6] has divided the electrodes into shorter sections to obtain greater sensitivity. The sections are connected by stub transmission lines that provide a phase delay of 360° minus the phase error introduced by each short electrode section. As in reference 5, the average phase velocity of the modulating signal is kept equal to that of the optical signal, but the shorter sections improve the sensitivity. However, as the sensitivity is increased by adding more sections, the bandwidth about the design frequency is decreased. This is also true of the Alferness method.

Our technique also divides the modulator into sections which limit the phase error per section. Now the individual sections are connected to surface antennas, as shown in Figure 1. The antennas are illuminated by a plane wave (the modulating signal) at an angle which provides the required phase-shift between modulator elements. Since $LiNbO_3$ has a high value of ϵ_r the antennas are much more sensitive to radiation incident from inside the substrate than from outside [7]. The required angle of incidence for the plane-wave illumination is $\theta = \sin^{-1}(n_o/n_m)$ where n_o is the optical refractive index and n_m is the microwave refractive index of $LiNbO_3$. The addition of more modulator sections does not affect the bandwidth in this case, as the bandwidth is simply that of a single antenna-plus-transmission-line section.

Since no physical connections are made to the antennas, and the short modulating elements need not be terminated by matched loads (although they could be), no parasitic circuit elements (such as bond wires or connectors) are introduced which might limit the possibility of scaling to higher frequencies. The limits would be imposed by the size of the optical waveguide and by the absorption spectrum of the $LiNbO_3$ itself [8]. A modulator at 500 GHz should be quite practical (Figure 2). In addition, at these very high frequencies the attenuation per unit length in the modulating electrodes can be very high. In the antenna-coupled modulator the problem of attenuation of the modulating signal as it propagates from section to section does not exist, since the elements are driven "from the side", in parallel rather than in series. Since the number of modulator sections required would be large, the antenna-coupled modulator's bandwidth advantage becomes important also. In exchange for these advantages, we must develop efficient means for illuminating the modulator.

III. ILLUMINATION OF THE ANTENNAS

We considered various possible methods of illuminating the antennas. The most obvious method is to cut a piece of dielectric as a wedge with the angle required for phase-velocity matching and launch the modulating signal into it from a feedhorn on the end of a metallic waveguide (Figure 3a). Another possibility is to mount the modulator longitudinally in a dielectric-filled waveguide, and adjust the waveguide dimensions so that the phase-velocity in the waveguide has the necessary value (Figure 3b). A third proposed method was to cut the $LiNbO_3$ to a small size, so that it could act as a dielectric waveguide for the modulating signal. If the dimensions of this

dielectric waveguide were correct, the phase velocity of the modulating signal could be adjusted to be the same as the phase velocity of the light propagating in the optical waveguide. The modulating power could be coupled into the modulator from another dielectric waveguide positioned alongside as a directional coupler (Figure 3c). This last approach seemed to be the most elegant one.

Unfortunately the most elegant solution also proved to be impractical. The dimensions of the piece of $LiNbO_3$ required for a W-band r .odulator would be 0.15 x 0.6 x 20 mm approximately. This would be impossibly fragile. The phase-velocity-matched dielectric-filled waveguide idea required that the waveguide be very near cutoff in order to match the phase velocities. A waveguide near cutoff is very dispersive, so the bandwidth of such a device would be inherently limited. The $LiNbO_3$ dielectric waveguide idea also suffered from this limitation. Also, a dielectric-filled metal waveguide, as in Figure 3b, is not the easiest thing to manufacture at W-band. Its transverse dimensions would be about 0.18 x 0.36 mm.

The most practical solution was to use the quasi-optical approach of Figure 3a, relying purely on geometry to match the phase velocities. This has the advantages of true time-delay phase matching, potentially very large bandwidth, and practical dimensions. The major disadvantage is that it is difficult to avoid having reflections from the $LiNbO_3$ - air interface propagate inside the feed. This can be overcome in part by putting a matching dielectric on the other side of the $LiNbO_3$, but this reduces the gain of the antennas.

IV. EFFECT OF THE DIELECTRIC INTERFACE ON THE ANTENNA PATTERN

The antenna pattern of an antenna at the interface between two dielectrics is very different from the pattern of the same antenna in one or the other of the dielectrics. The effect of the $LiNbO_3$ - air interface can best be visualized by assuming that the antenna is initially entirely in air. The $LiNbO_3$ interface is brought in slowly from some distance away. The pattern in the air is now composed of the original pattern plus the superimposed pattern reflected by the interface. The pattern of an antenna on the interface results when the distance to the interface goes to zero. The pattern in the $LiNbO_3$ can be computed in a similar way. As a result of the interface, the antenna

pattern is strongly altered.

Figure 4 shows the effect on the H-plane pattern of an infinitesimal dipole. For an infinitesimal dipole in air the H-plane pattern is a simple circle. On an interface this circle becomes distorted as shown. There is no radiation along the interface. The radiation into the air is very weak, so that the radiation into the dielectric is dominant. For dielectric constants greater than 4 the antenna essentially couples into the dielectric only. The superposition of the direct and reflected radiation gives the pattern inside the dielectric a peak at the critical angle.

It is relatively straightforward to compute the antenna pattern of a long thin dipole on the interface by assuming a current distribution on the antenna. The effective wavelength (which determines the current distribution) at the surface is determined by the average of the dielectric constants on either side. The antenna patterns of other types of antenna on the interface are more difficult to compute. Dipoles, of course, are resonant antennas, which limits their bandwidth. Other antennas are known to have broader bandwidth, such as bow-tie antennas, spiral antennas and log-periodic antennas. Unfortunately their properties on a dielectric interface have not been studied extensively. The spiral antennas are not useful in the modulator context because they enclose their terminals in the spiral. Consequently there is nowhere to put the modulator electrodes. Log-periodic antennas are of limited application because they are so big that they are difficult to position close together (Fig. 5). This would mean having to position the modulator electrode sections at long intervals along the optical waveguide, which is an inefficient use of the real-estate. To date the dipole antennas and bow-tie antennas seem the most useful. The dipoles are well-understood, which simplifies design and allows for comparison of results with theory. Also, the resonant nature of the dipoles can be used in the design to increase modulator sensitivity at the center frequency. The bow-ties should allow for significantly broader bandwidth, but with less sensitivity. In addition, the ends of a bow-tie antenna have little effect on its performance, so that it is possible to connect bias leads there. (Bias is usually necessary in Mach-Zehnder amplitude modulators to achieve the optimum operating point.) It may be possible to design antennas which have gain in the desired direction, perhaps by designing a V-antenna. However there has been very little work to date on directional interfacial antennas whose main beam is not straight into the dielectric.

V. THE MODULATOR ELECTRODES

The modulator electrodes may be terminated or unterminated. Early electro-optic modulators used unterminated electrodes. The problem with these was that the electrodes were, in effect, capacitors and this caused the response to roll off at high frequencies when the capacitive impedance became less than the source impedance. This problem was overcome by designing the electrodes to act as transmission lines with the same characteristic impedance as the source impedance. The electrodes were matched at the other end, and so presented the source with a matched impedance at all frequencies. These so-called traveling-wave modulators suffered a 6 dB loss in DC sensitivity but enjoyed a dramatic increase in bandwidth - the new limitation was the phase-velocity mismatch problem we have already discussed.

In our application we considered using terminated transmission lines for the same reasons, but elected not to do so. There were two reasons for this. One was the loss in sensitivity. The other was the fact that matched terminations do not scale very well. Fabricating a matched load for a coplanar strip transmission line at 100 GHz would be a difficult and uncertain proposition, and we would need one for every antenna/transmission-line element in the modulator.

The use of unterminated transmission lines brings two disadvantages. One is the resonant behavior of such lines, which limits bandwidth. This is what caused the problems in the early electro-optic modulators. The other is the fact that there is now more than one electrical wave propagating on the electrodes, so that there is more than one electrical wave interacting with the optical signal. The modulating wave propagates down the electrodes, finds an open circuit at the end and reflects back. This then reflects from the mismatch at the antenna, and so on. The forward waves can be combined as one single forward-propagating wave on the electrodes, and the backward waves can be combined similarly. The forward wave interacts much more strongly with the optical signal because it has a much smaller phase-velocity mismatch. Since the backward wave is propagating in the opposite direction to the light, it interacts more weakly. Nevertheless, the backward wave does modify the interaction strength as a function of frequency. At low frequencies the two waves produce voltages which add all along the line, producing 6 dB more response than a terminated line (no surprise!). Even ignoring the impedance problems, as the frequency increases the response rolls off

more quickly for the unterminated line (Figure 6). The theory is detailed in Section IX below.

Despite these disadvantages, the unterminated line is scaleable, and this was most important. Its frequency response is not a big problem, because the modulator elements can be made short as required. Also, since it has resonances, if the antenna is a dipole the resonances can be used to match the dipole and peak the responsivity at the design frequency.

VI. NUMBER OF SECTIONS - IS N BETTER THAN 1 ?

At first glance it is not immediately obvious that increasing the number of modulator elements is any advantage, since the existing power is divided among them. That is, it is not clear whether it is better to have one modulator element driven with all the power, or many modulator elements with the power split between them. Obviously the antenna-driven modulator-element array only makes sense if it is better than a single modulator. It is, in fact. Due to the phase-velocity mismatch, the length of a single modulator element is limited. There is an optimum length, beyond which things get worse. Suppose such an optimal modulator element is driven with 1 Watt, and produces a phase deviation θ. Now if N of these modulator elements are driven with 1/N Watt each, the phase deviation produced by each one is $\theta/\sqrt{N}$ because the phase deviation depends on the voltage, i.e. on the square root of the power. Since there are N of these modulator elements, they produce a total phase deviation of $\sqrt{N}\ \theta$. This means that N modulator elements can be used to make a modulator which is $\sqrt{N}$ times more sensitive than a single-element modulator.

This suggests that the number of antenna/electrode elements should be increased without limit. However, we have assumed perfect phase-velocity matching. As the number of antennas increases the antenna array becomes longer and the phase-velocity-matching requirements become increasingly stringent. Phasefront curvature of the modulation signal must be very small, and the angle of incidence must be very precise. Small errors can eliminate all the advantages of a large value of N, and can even make the large-N case worse than the small-N case. In practice a modulator more than a couple of cm long at W-band imposes difficult illumination requirements. Nevertheless, a modulator this long is still much longer than any possible single-section modulator at

this frequency.

In general the performance of a modulator depends on the phase-velocity mismatch, the signal attenuation in the electrodes, the electrode structure and the distribution of the signal power. The various optimization considerations are explored further in the Appendix.

VII. X-BAND PROTOTYPE MODULATOR

Figure 7 shows the mask for an X-band prototype modulator. There are five antenna/modulator sections. The overall length is 25 mm. The antennas are "two half-waves in phase" dipoles, and the modulator sections are approximately a half-wave long at 12 GHz, based on an assumed effective microwave surface refractive index of 3.8 (i.e. the dielectric constant is taken as the mean of the dielectric constants of air and $LiNbO_3$). This electrode pattern was positioned over a straight section of optical waveguide to produce a phase modulator rather than a Mach-Zehnder amplitude modulator, but the same mask would also work if applied to one arm of a Mach-Zehnder. The 6μm optical waveguide was produced by in-diffusion of titanium.

The microwave feed used to drive the modulator is shown in Figure 8. The $LiNbO_3$ substrate is attached to a wedge of Stycast ^{R} dielectric with ϵ_r=30, and the signal is matched into this material by two matching layers of intermediate dielectric constant. The wedge angle is 23° to match the microwave and optical phase velocities: a wedge is necessary because the critical angle for a material with ϵ_r=30 is only 9°, making it impossible to couple into a flat substrate at any larger angle. The peak response of the dipole antennas is in the direction of the critical angle: the response in the 23° direction is only approximately 1 dB less (Figure 9). The optical beam is coupled into and out of the optical waveguide using microscope objectives. Optical damage occurs in the guide at the 633 nm optical wavelength used, and optical power was limited because of this. Typically we used 1/2 mW of optical power from the HeNe laser.

The phase modulated signal cannot be detected using a photodetector. We used a scanning Fabry-Perot interferometer to show the existence of modulation sidebands and measure their amplitude. The phase deviation introduced by the modulator can be

deduced from the amplitude of the sidebands relative to the carrier (for small phase deviation) from the formula [9]

$$\Delta\phi = 2\sqrt{\frac{P_{sideband}}{P_{carrier}}}$$

It is more usual to build an amplitude modulator and detect the signal directly, but the above method is simple and has the advantage that it works at much higher modulation frequencies, where (AM) photo detectors are scarce. It has one notable disadvantage, however. The frequency spectrum is aliased by the scanning Fabry-Perot at frequency intervals equal to the free spectral range, so that sidebands which are an integral number of free spectral ranges off carrier are lost behind an aliased version of the carrier.

Figure 10 shows the modulator response as a function of frequency. The response is here defined as phase deviation normalized to the square root of the drive power, in units of "degrees per root Watt". This measure is linearly related to "degrees (or radians) per Volt", which is the common measurement when direct connections are made and voltage can be measured directly. There are no data points at 6, 8, 10 and 12 GHz due to the aliasing of the carrier at 2 GHz intervals which obscured the sidebands on the oscilloscope display. The graph shows straight-line interpolation between the data points.

The modulator was operated with a number of different wedge angles to establish the effect of the illumination angle on performance. This may be modeled by considering the pattern of each antenna alone, the pattern of a phased array of such antennas (with the light in the optical waveguide doing the phasing), and the pattern of a phased array of antennas with unequal illumination. Figure 11 shows the patterns of arrays of 3, 4 and 5 equally illuminated antennas. We have included the smaller numbers of antennas because the antennas at either end of the modulator may be poorly illuminated. If a cosine distribution across the five antennas is assumed, the result is not unlike the 4-antenna case. Also plotted in Figure 11 is the experimental response of the prototype modulator, averaged over the 9-12 GHz band at each angle of incidence. The response peaks at about 23° as expected, confirming the phase-velocity-matching picture. The absence of the null in the experimental data is probably due to the multiple reflections inside the wedge.

VIII. V-BAND PROTOTYPE MODULATOR

A V-band phase modulator was designed based on scaling of the X-band prototype. The mask is shown in Figure 12 (there were four antenna arrays of slightly different dimensions on each chip). Essentially the design of each antenna/modulator element is based on a direct scaling of the original prototype, except that the electrode gap size is fixed, and this fixes the lateral dimensions of the electrodes. The antennas were approximately 1mm long (end-to-end), and the electrodes were 0.74 mm long. The electrode gaps were 8μm.

Since the mm-wave waveguide from which the modulating signal originates is now much smaller, while the antenna array is still long (more antennas), a different microwave feed is needed. The modulating signal is coupled from WR-15 waveguide into a tapered teflon slab waveguide 1.5 mm thick. This tapered slab provides a means of expanding the wave to the dimensions of the antenna array, which was 1 x 18 mm. Using a single quarter-wave layer, the power is matched into a slab of $LiNbO_3$ which is cut as a wedge to provide the correct angle of incidence for the modulating signal. The microwave feed is shown in Figure 13. The phase deviation was again measured using the scanning Fabry-Perot method, which works just as well with mm-wave as with microwave modulation. However we did not have complete confidence in the accuracy of our mm-wave power measurements (made with a K-band power-meter), and so can give only approximate results in terms of degrees of phase deviation per $\sqrt{\text{Watt}}$. These results are shown in Figure 14.

IX. DISCUSSION OF RESULTS

The structure in the frequency response arises from many sources: antenna and electrode resonance; reflections within the wedge; nonideal input matching layers; etc. However, we have found that the general shape of the X-band prototype modulator response is accounted for quite well by a model of the antenna/electrode impedance variations and the frequency response of the individual modulators. In this model the electrodes are treated as lossless transmission lines, open-circuit at the end; the antenna is treated as a lossy transmission line (the loss represents radiation effects); and the individual modulators have a frequency response basically determined by the well-

known sinc-function response, except that there are two sinc terms, one for the forward-propagating wave at the modulation frequency and one for the wave reflected back from the open circuit at the end of the modulator electrodes.

The antenna impedance is modeled as the impedance of a lossy transmission line with an open-circuit termination:

$$Z_{ant} = \frac{95}{\tanh(0.157\,\theta + j\,\theta)}$$

where θ is the electrical half-length of the antenna. This expression is based on an extension of the results of Kominami et al [10].

The electrodes are treated as lossless transmission lines with open-circuit termination. The input impedance of such a line is

$$Z_{in} = \frac{Z_o}{\tan \zeta}$$

where ζ is the electrical length of the transmission line in radians.

The amplitude of the forward-traveling component of the standing-wave on the electrode is then given by

$$V_{fwd} = \frac{Z_o \sqrt{P \cdot R}}{\sqrt{R^2 \sin^2\zeta + \{ X \sin \zeta - Z_o \cos \zeta \}^2}}$$

where P is the power which the antenna could deliver to a matched load,
R is $Re\{ Z_{ant}\}$
X is $Im\{Z_{ant}\}$

Of course the reverse-propagating wave has the same amplitude. The received power varies with the effective area of the antenna, which is a function of frequency. Across the X-band the variation is quite slow. Over a wider range it is possible to compute the effective area; however this computation is very tedious. Simpler estimates of the effective area based on the antenna's H-plane beamwidth at various frequencies produced an approximation which was used in the model. This approximation was

$$A_{eff} \sim 29 - \lambda + 0.028\,\lambda^2$$

where λ is the free-space wavelength of the modulating signal.

These two waves then interact with the light in the optical waveguide. Since one wave is propagating in the same direction as the light, it interacts more strongly with the optical wave than the signal wave propagating in the reverse direction. The total interaction is given by

$$\delta(f) = 0.5\,L \left\{ \frac{\sin[\frac{\pi f}{c}(n - n_m)L]}{[\frac{\pi f}{c}(n - n_m)L]} + \frac{\sin[\frac{\pi f}{c}(n + n_m)L]}{[\frac{\pi f}{c}(n + n_m)L]} \right\} V_{fwd}\, A_{eff}$$

where
- $\delta(f)$ is proportional to the modulation index
- L is the length of a single modulator section
- f is the frequency
- c is the speed of light (2.998×10^8 m/s)
- n is the refractive index of $LiNbO_3$ at the optical frequency (2.25 approx.)
- n_m is the effective refractive index to the modulating signal (3.8 approx.)

The frequency response which is predicted by this simple model of impedances, modulator element frequency response and antenna gain is shown in Figure 15. It agrees remarkably well with the general shape of the experimentally determined response of the X-band prototype (Figure 10).

The peak around 12 GHz occurs when the modulator elements are a half wave long, at which point the antennas are approximately two half-wavelengths long. The antenna driving-point impedance and the modulator element input impedance are then both high. At 6 GHz there is another peak when the antenna is a half-wave long and the modulator element has a low input impedance. The lower-frequency peak also benefits from the increased modulator sensitivity at lower frequencies - the modulator electrodes are electrically shorter and the sinc terms are nearer to unity. (It was necessary to use WR 137 waveguide to measure this lower-frequency peak, so the microwave feed

geometry was changed somewhat.)

Peak response values exceed 100 degrees per $\sqrt{W}$. This compares favorably with conventional microwave modulators (Erasme et al. [11] report a peak response of 131 degrees per $\sqrt{W}$ for their phase-reversal travelling-wave modulator, operating at a wavelength of 1153 nm - note that sensitivity varies as $1/\lambda_{optical}$). This is only achieved over a narrow band, but is encouraging in a prototype. The narrow bandwidth results from the use of simple resonant elements. Other antenna designs with broadband elements will likely result in a flatter frequency response. Of course even here there is a region between the two peaks which is quite flat, but less sensitive by about 10 dB.

X. FUTURE DEVELOPMENTS

To date we have demonstrated that the antenna-coupled modulator is capable of efficient mm-wave modulation of optical signals. However, the structure used had a relatively narrow bandwidth and was not ideally suited for use as part of a Mach-Zehnder amplitude-modulator structure. The Mach-Zehnder design requires a DC bias to ensure that the modulation drives the interferometer in its most linear (and most sensitive) region. There is no good way to connect DC bias leads to simple surface dipoles. A new modulator has been designed to overcome these two difficulties and is being fabricated at present (Figure 16). This new modulator uses bow-tie antennas in place of the dipoles. The bow-ties approximate frequency-independent structures, and this should allow much greater bandwidths. In addition the ends of the bow-ties interact only weakly with the radiation field and can be used as bias leads with little effect on RF performance. There is some sensitivity penalty associated with the use of these antennas, since the peaking of the response which was due to the dipole resonances is lost. The new modulator is designed to operate as a Mach-Zehnder amplitude modulator over the range 60-94 GHz. We also propose to demonstrate operation at 1.3 μm and/or 1.5 μm optical wavelengths.

The theory of antennas on dielectric substrates is not very well developed, although dipoles are well understood. Further developments in this area will be applicable to these modulators. Improved waveguide-to-antenna coupling is also desirable. Demonstrations at significantly higher modulation frequencies would depend very much on the availability of mm-wave or sub-mm-wave power sources.

XI. ACKNOWLEDGEMENTS

The authors wish to acknowledge the invaluable assistance of James H. Schaffner and Robert L. Joyce of Hughes Research Laboratories, who fabricated the modulator chips used in this work, and the technical assistance of Reynold E. Johnson at Caltech in the experimental measurements.

XII. REFERENCES

[1] William B. Bridges, Finbar T. Sheehy and James H. Schaffner, "Wave-Coupled $LiNbO_3$ Electrooptic Modulator for Microwave and Millimeter-Wave Modulation," IEEE Photonics Technology Lett. Vol. 3, No. 2, pp. 133 - 135, February 1991

[2] – , "Velocity-Matched Electro-Optic Modulator," SPIE Vol. 1371 High Frequency Analog Fiber Optic Systems (1990) pp. 68-77, San Jose, California, September 1990

[3] G. E. Betts, L. M. Johnson, and C. H. Cox, III, "High-Sensitivity Lumped-Element Bandpass Modulators in $LiNbO_3$," IEEE J. Lightwave Tech., Vol. 7, pp 2078-2083, December 1989.

[4] C. M Gee, G. D. Thurmond, and H. W. Yen, "17-GHz Bandwidth Electro-Optic Modulator," Appl. Phys. Lett., Vol. 43, pp 998-1000, December 1983.

[5] R. C. Alferness, S. K. Korotky, and E. A. J. Marcatili, "Velocity-Matching Techniques for Integrated Optic Traveling Wave Switch/Modulators," IEEE J. Quant. Electron. QE-20, pp 301-309, March 1984.

[6] J. H. Schaffner, "Analysis of a Millimeter Wave Integrated Electro-optic Modulator with a Periodic Electrode," Paper 13 at SPIE OE-LASE Conference 1217, Proceedings, pp 101-110, Los Angeles, Calif., January 16-17, 1990.

[7] N. Enghetta, C. H. Papas, and C. Elachi, "Radiation Patterns of Interfacial Dipole Antennas," Radio Science, Vol. 17, pp 1557-1566, Nov.-Dec. 1982.

[8] Handbook of Optical Constants of Solids, Edward D. Palik, Academic Press 1985

[9] See, for example, Reference Data for Radio Engineers, 5th Ed., Howard Sams, New York, 1968, Sec. 21-7.

[10] Masanobu Kominami, David M. Pozar and Daniel H. Schaubert, "Dipole and Slot Elements and Arrays on Semi-Infinite Substrates," IEEE Trans. Ant. & Prop. AP-33, No. 6, June 1985

[11] D. Erasme, D. A Humphries, A. G. Roddie, and M. G. F. Wilson, "Design and Performance of Phase Reversal Traveling Wave Modulators," IEEE J. Lightwave Tech., Vol. 6, pp 933-936, June 1988.

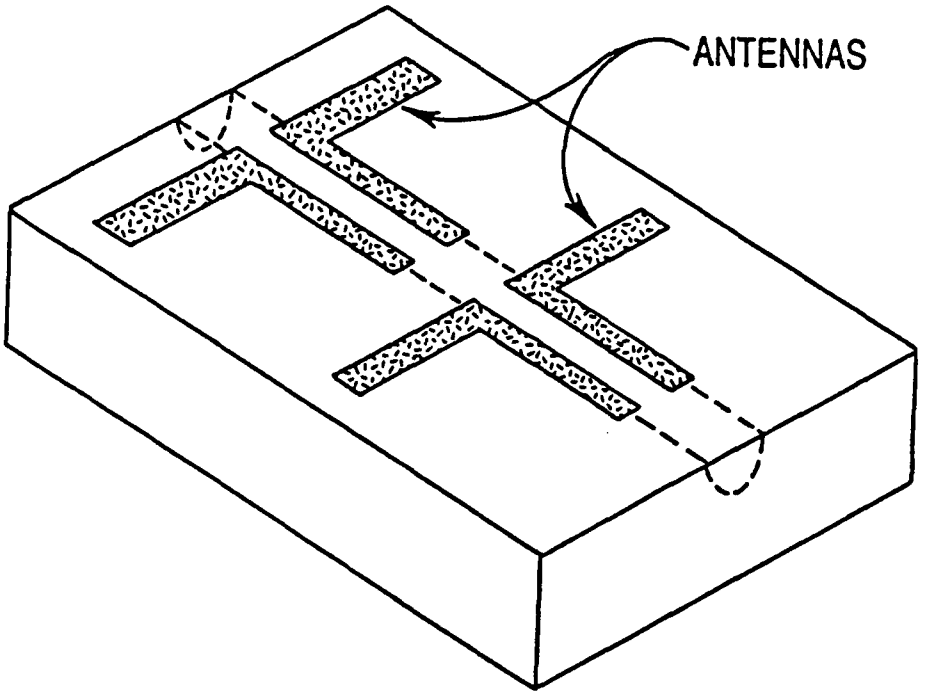

Figure 1: Schematic drawing of two dipole antennas and connected transmission line sections on the surface of a waveguide electro-optic modulator.

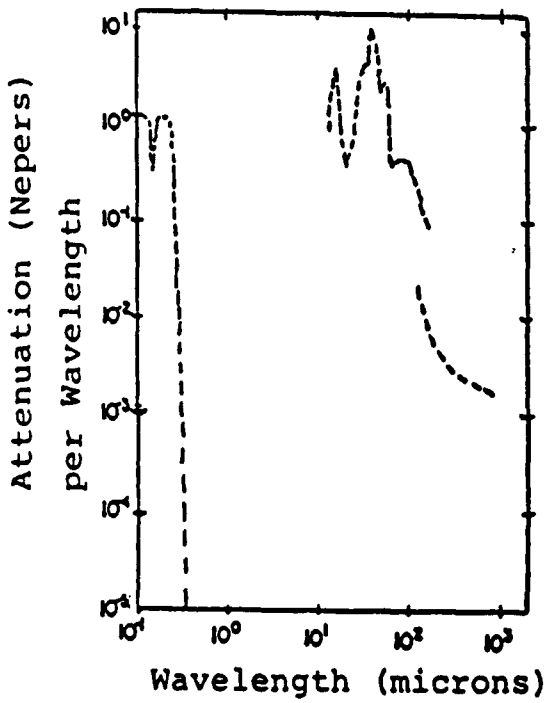

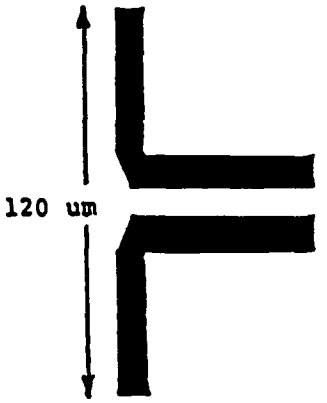

Figure 2: The absorption spectrum of $LiNbO_3$ and scaling of modulator elements show that a 500 GHz modulator is feasible.

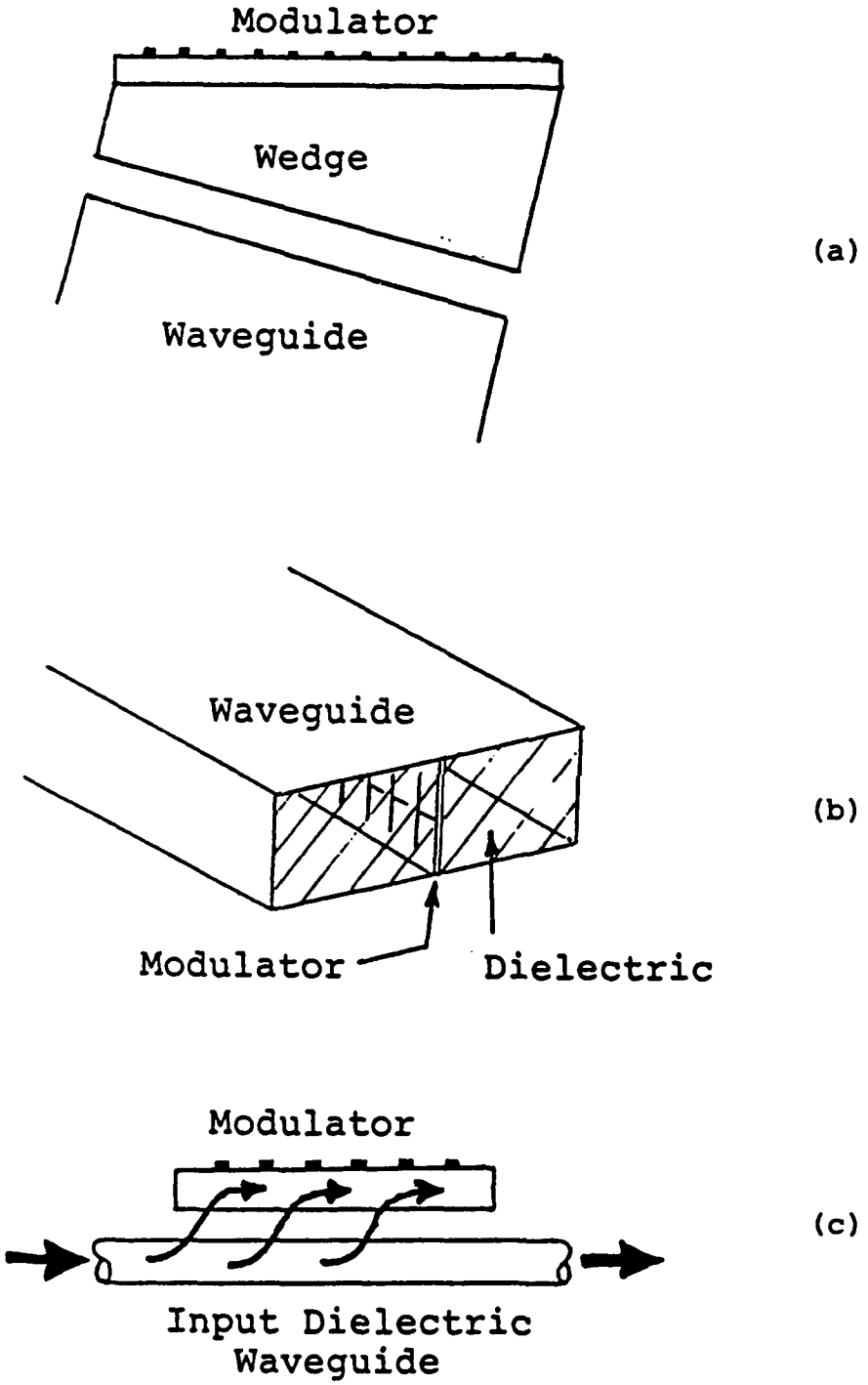

Figure 3: Phase-velocity matching concepts.

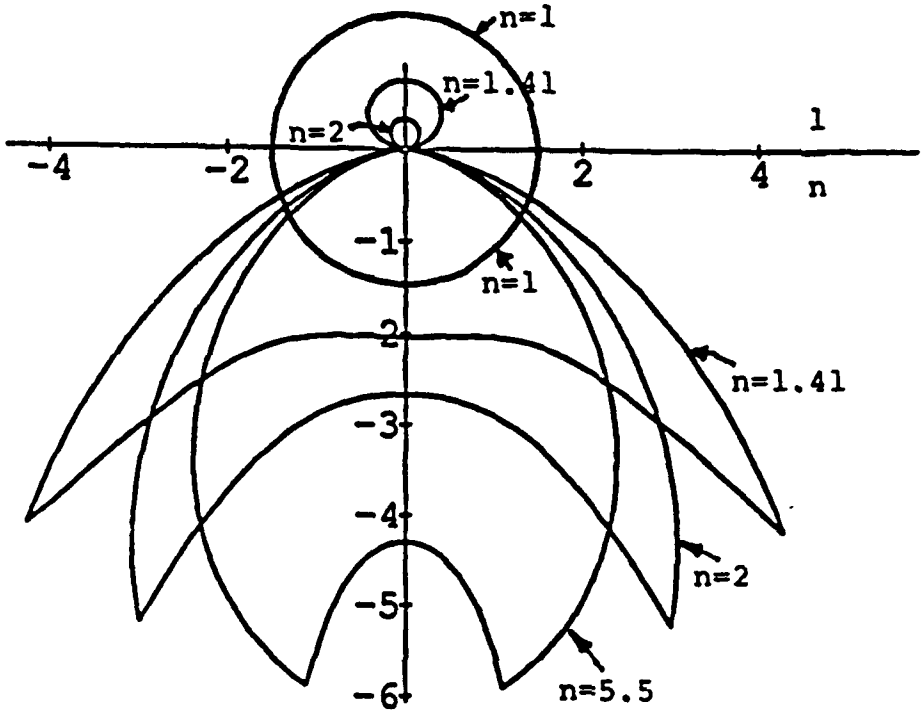

Figure 4: H-plane antenna patterns of an infinitesimal dipole on a dielectric interface.

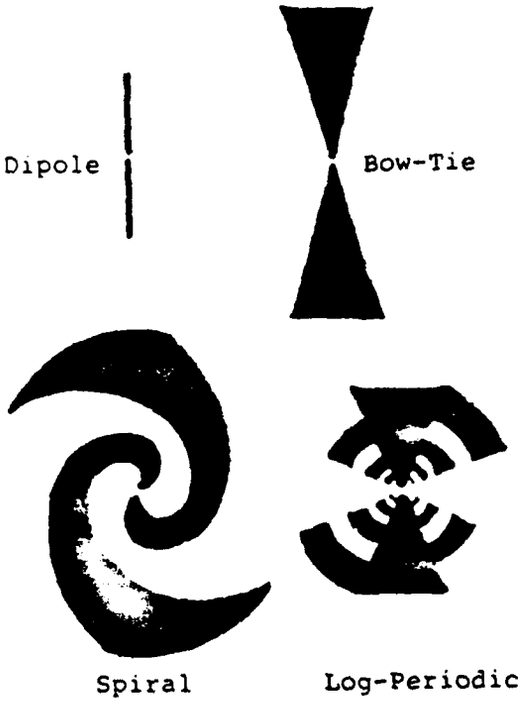

Figure 5: Types of Planar Antenna

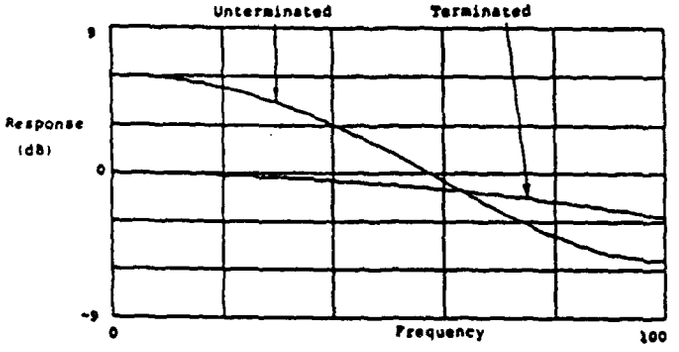

Figure 6. Terminated and Unterminated Electrodes

- Electrical Length is 360° at f=100

Impedance Match to Modulation Source Assumed.

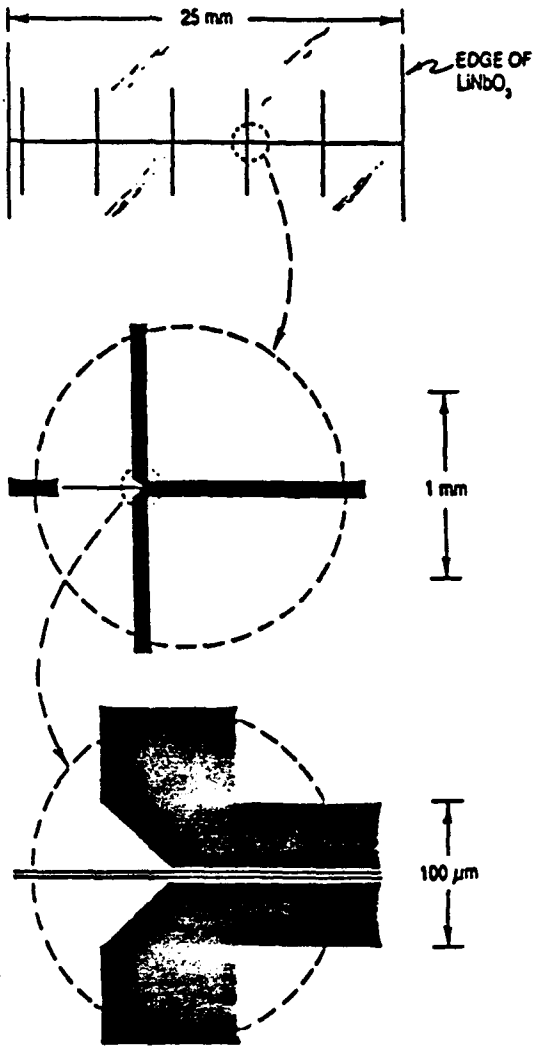

Figure 7: Photolithographic mask for 5 antenna plus transmission-line elements covering a 25 mm long optical waveguide. Magnified details are shown in the lower two drawings.

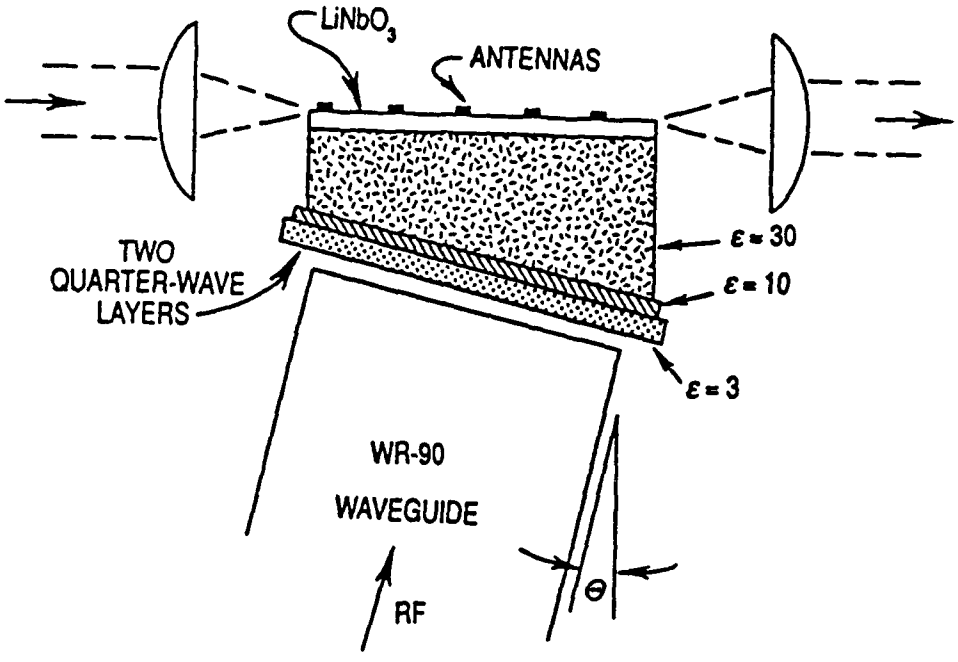

Figure 8: Schematic side view of an experimental modulator showing $LiNbO_3$ wafer with antennas, input and output lenses, wedged block of high dielectric-constant material, matching layers, and microwave waveguide.

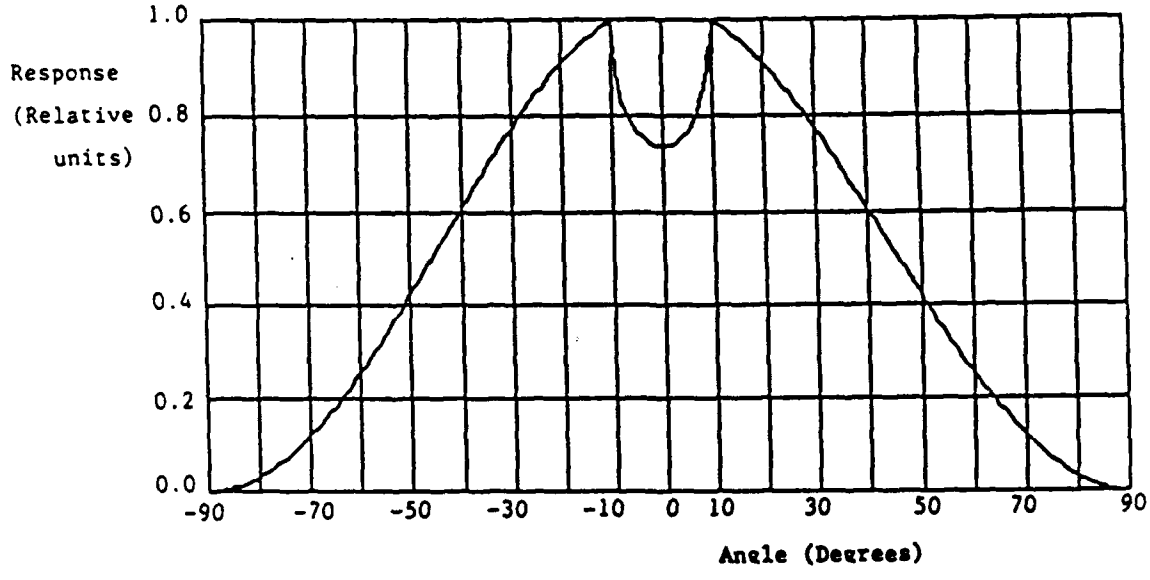

Figure 9: Antenna pattern of dipole on $LiNbO_3$. The critical angle is 9°, the phase-velocity-matching angle is 23°. Note the cusp-like behavior at the critical angle.

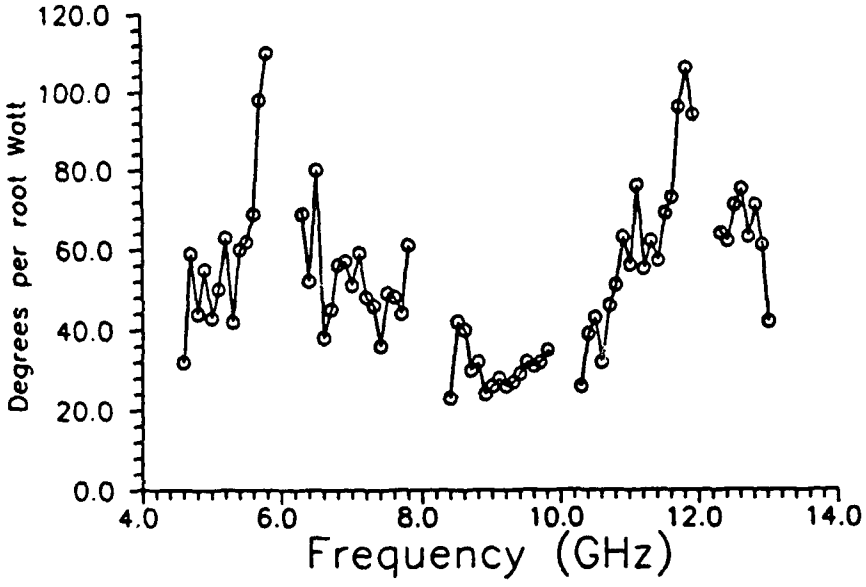

Figure 10: Frequency response of the experimental X-band modulator.

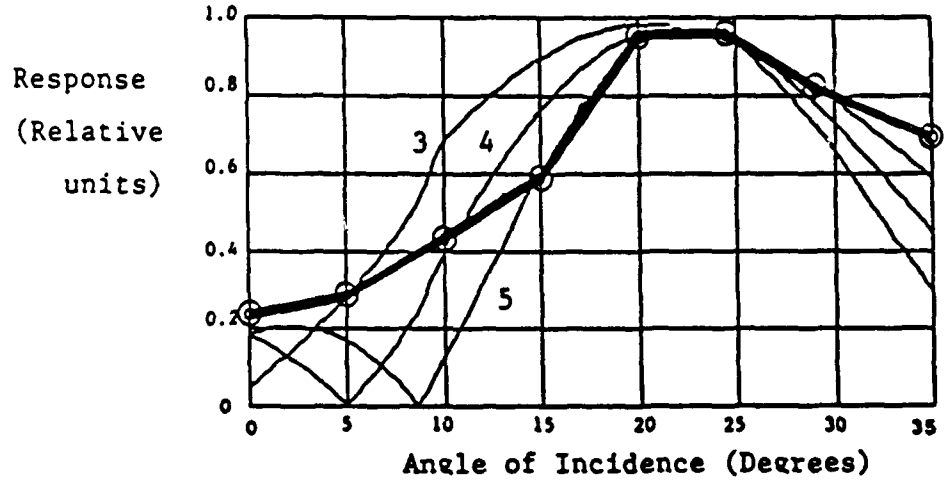

Figure 11: Effect of illumination angle on performance: theory for 3, 4, and 5 antennas, and results from experimental modulator.

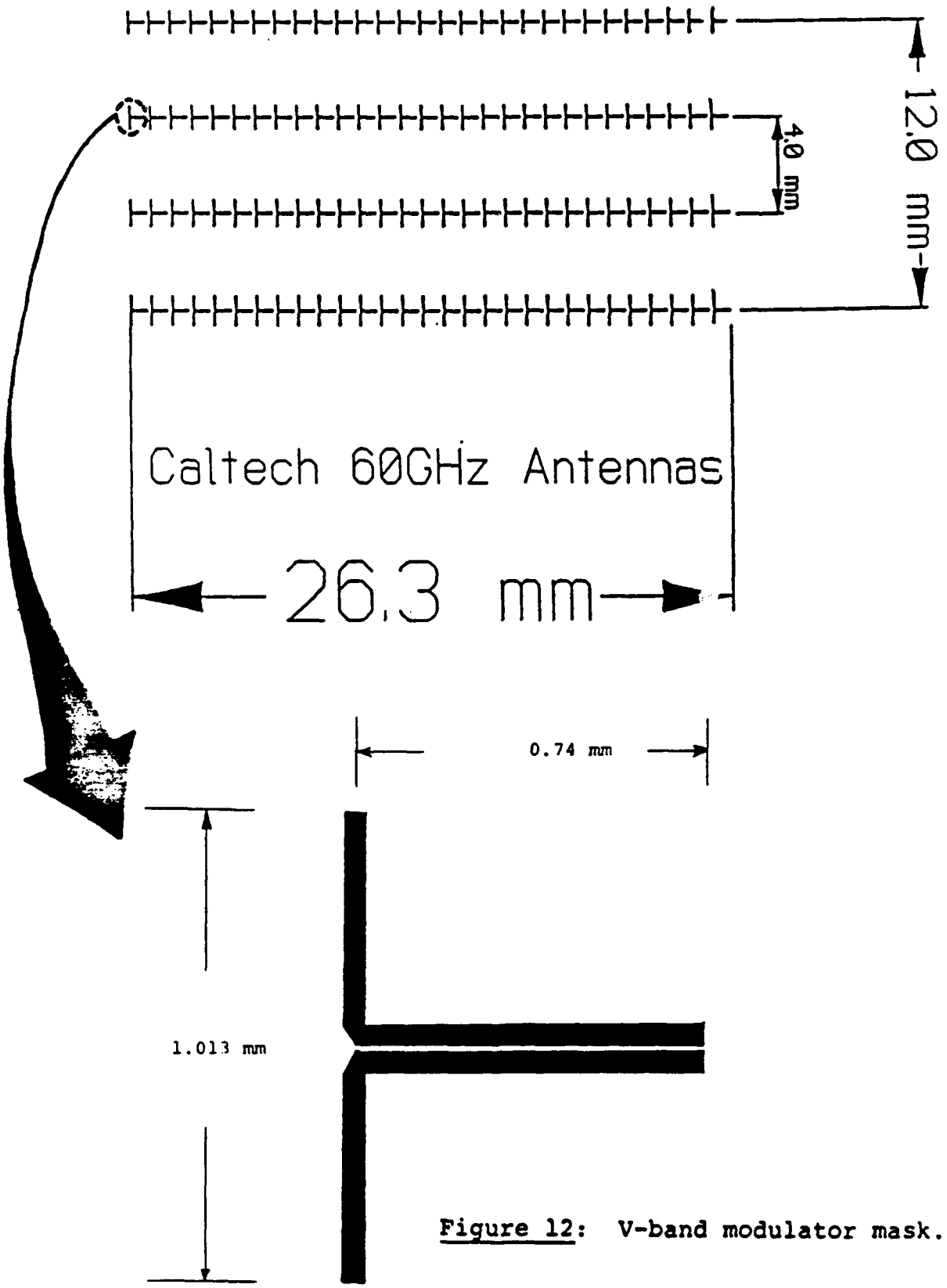

Figure 12: V-band modulator mask.

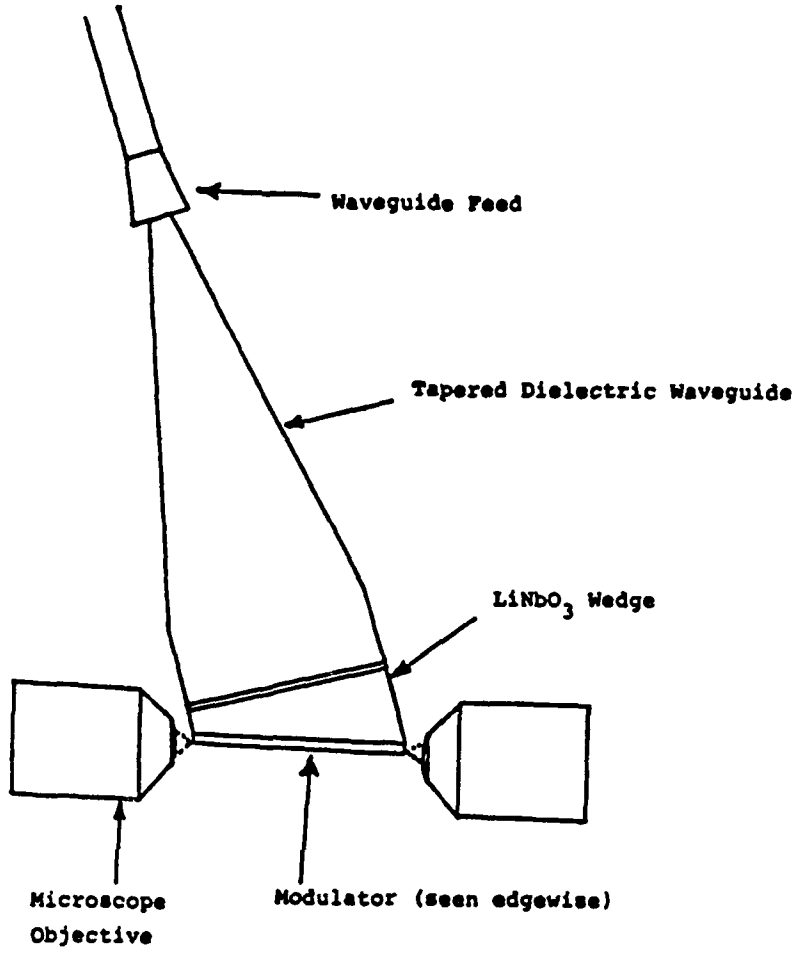

Figure 13: The V-band microwave feed.

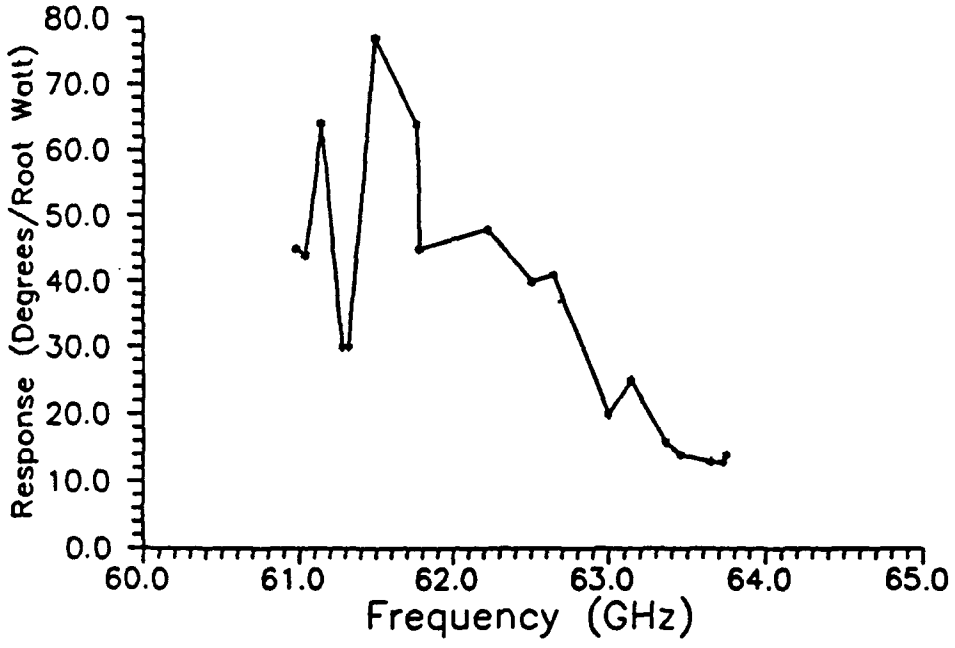

Figure 14: Frequency response of the prototype V-band modulator.

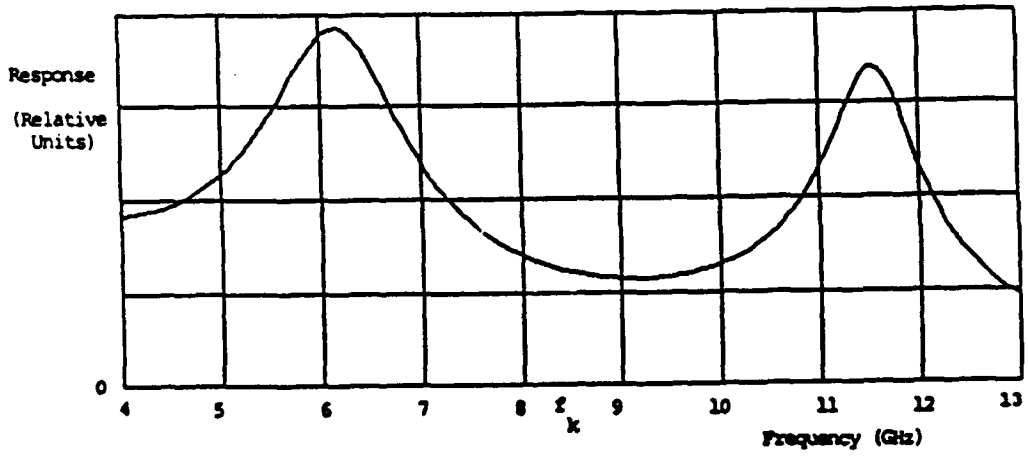

Figure 15: Frequency response predicted by simple model of impedances, modulator element frequency response, and antenna gain.

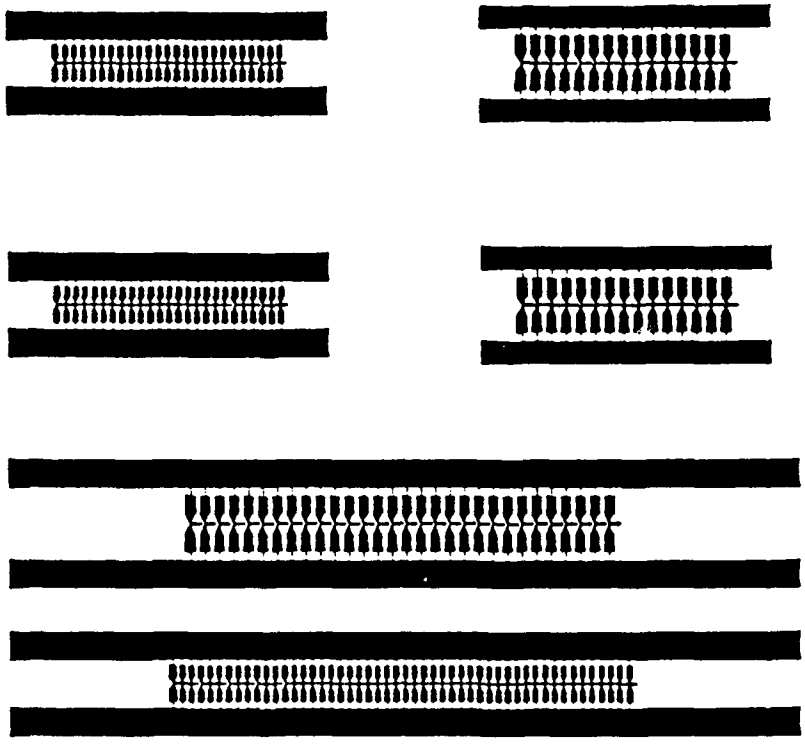

Figure 16: Mask for new broadband modulators designed for V-band and W-band operation.

APPENDIX

Optimum Power Distribution in Traveling-Wave Electro-Optic Modulators

1. Executive Summary

Traveling-wave modulators suffer from phase-velocity mismatch and transmission-line attenuation. Where high modulation sensitivity is required at a specific frequency, it may be optimal to split the modulator into a number of shorter elements, each driven with a fraction of the available modulation signal power. We show how to determine the optimum configuration in the case of a modulator which suffers from neither problem, in the case of a modulator whose element lengths are fixed by some constraint, in the case of a lossy modulator and in the case of a phase-velocity-mismatched modulator. In addition we examine the bandwidth implications of the various approaches.

2. Introduction

Traveling-wave electro-optic modulators are usually based on electro-optic phase modulators. The light propagates through a crystal whose refractive index depends on the modulating electric field strength. The output phase of the optical signal is thus controlled by the modulating field. At low frequencies the phase deviation produced varies linearly with the interaction length and with the applied electric field. If an amplitude modulator is required the modulated beam is interfered with another beam (which may be unmodulated or modulated in the opposite sense), converting phase modulation to amplitude modulation.

At high modulation frequencies there are two common problems with these modulators. First, the phase-velocity of the modulating signal may differ appreciably from that of the optical signal, causing the two to fall out of step within the interaction length. The optical phase then reflects a time-averaged version of the modulating signal. The second problem is that the attenuation of the transmission-line used to guide the modulating signal increases at higher frequencies, so that the modulating signal dies away after a short distance, reducing the effective interaction length.

In either case it may be possible to build a modulator which meets all required specifications at some design frequency except the sensitivity requirement. One could

consider using a number of such modulator elements cascaded to increase the output signal. This would mean dividing the available modulation signal power between the modulator elements. We examine some cases where this is an advantage, and note where it is not.

3. How to Split a Traveling-Wave Modulator

When splitting an amplitude modulator one can split the interaction region into a number of shorter sections, but not interfere the modulated beam with the unmodulated one until after the final phase-shifter. Alternatively one can split the modulator by making a number of complete amplitude modulators, each with the shorter interaction length. This latter approach introduces very severe distortion, which is hardly desirable.

Consequently we need only consider phase modulators. A phase modulator may be split into any number of subsections without affecting its distortion. If an amplitude modulator is required, one usually builds two phase modulators . When these are driven in opposite phases and their outputs are combined, the net output is an amplitude-modulated signal.

4. The Definitions

Referring to Figure 1, the modulator consists of N modulator elements. The fraction of the total modulation signal power delivered to the k^{th} element is P_k. The phase contribution of a modulating element may be written as

$$\phi(P) = a\, P^{1/2} \qquad (1)$$

where a depends on the details of the modulator.

5. Ideal Modulator Elements

An ideal modulator element is one which is not affected by phase-velocity mismatch or attenuation. It makes a phase contribution

$$\phi(L,P) = Q\, P^{1/2}\, L \qquad (2)$$

where P is the modulation signal power,
L is the interaction length,
Q is a constant.

The modulator is to be constructed of a number N of these modulator elements.

The modulating signal power is split between the elements so that the k^{th} element is driven with P_k. The interaction length of the k^{th} element is L_k. Then

$$\phi = \sum_k Q\, P_k^{1/2}\, L_k \tag{3}$$

$$L = \sum_k L_k \tag{4}$$

$$P = \sum_k P_k \tag{5}$$

The goal is to maximize ϕ for given values of L and P. Consider the N^{th} and $(N-1)^{th}$ modulator elements. Suppose their combined length is L_c and their combined power is P_c. Their combined phase contribution is ϕ_c. Then

$$L_{N-1} = L_c - L_N \tag{6}$$

$$P_{N-1} = P_c - P_N \tag{7}$$

$$\phi_c = Q\,[\,(P_c - P_N)^{1/2}(L_c - L_N) + P_N^{1/2}\, L_N\,] \tag{8}$$

The maximum of this function occurs at two endpoints, where

either $\quad P_N = P_c \quad L_N = L_c \tag{9}$

or $\quad P_N = 0 \quad L_N = 0 \tag{10}$

So the best thing to do is to use just one long modulator element (driven with all the power) in place of the two original elements. The modulator now has (N-1) modulator elements. By induction from this, the global optimum is a single modulator element with length L, driven with all the available modulation signal P. Both L and P should be as large as possible, but increasing L is more effective than increasing P.

6. Length-Limited Modulator Elements

If the maximum length of a single modulator element is fixed by some constraint, the optimum configuration changes. For example, phase-velocity mismatch means that there will be an optimum length for each modulator element, so that if the length of a modulator element is increased beyond a certain value the phase contribution actually begins to decrease. Suppose a modulator is to be constructed using modulator elements, each of which has this optimum length. Then

$$\phi = \sum_{k=1}^{N} Q\, L\, P_k^{1/2} \qquad (11)$$

where $$P = \sum_{k=1}^{N} P_k \qquad (12)$$

The maximisation now amounts to finding the maximum of

$$\sum_{k=1}^{N} P_k^{1/2} \qquad (13)$$

which occurs when $P_k = P/N.$ (14)

The optimum occurs when the power is distributed equally between the modulator elements. Its value is

$$\phi = Q\, L \sqrt{P}\, \sqrt{N} \qquad (15)$$

It is obvious from this that the more modulator elements are involved the better. So, when there is an optimum *length for a single modulator element* but they can be combined to make a better modulator, the best approach is to use as many modulator elements as possible and to split the power equally among them. The improvement thus obtained varies as $\sqrt{N}$.

7. Loss-Limited Modulator Elements

Transmission-line loss may be the effect which limits the useful length of the modulator. The attenuation of the modulating signal in the transmission-line makes each additional unit of transmission-line length less effective. Nevertheless, there is no optimum line length. It should still be made as long as possible.

However, it may be more effective to split this length equally between N modulating elements. This would also involve splitting the available modulation drive power, of course.

If the attenuation on the transmission-line is α, then the phase contribution from the k^{th} modulator element is

$$\phi_k = Q\left(\frac{P}{N}\right)^{1/2} \int_0^{L/N} e^{-\alpha x}\, dx \qquad (16)$$

$$= Q\left(\frac{P}{N}\right)^{1/2} \frac{1}{\alpha} \left[1 - e^{-\alpha L/N}\right] \qquad (17)$$

The total phase contribution is then

$$\phi = N\,\phi_k = \frac{Q\sqrt{P}\sqrt{N}}{\alpha}\left[1 - e^{-\alpha L/N}\right] \qquad (18)$$

Observe that the correct number of sections to use is N when

$$\sqrt{N\text{-}1}\ \left[1 - e^{-\alpha L/(N-1)}\right] \le \sqrt{N}\left[1 - e^{-\alpha L/N}\right] \le \sqrt{N+1}\ \left[1 - e^{-\alpha L/(N+1)}\right] \qquad (19)$$

The number of sections to use is implicitly defined as a function of (α L). The optimum values are listed in Table 7.1.

αL (nepers)	αL (dB)	N
0 - 1.76	0 - 15.3	1
1.76 - 3.07	15.3 - 26.6	2
3.07 - 4.34	26.6 - 37.6	3
4.34 - 5.6	37.6 - 48.6	4
5.6 - 6.9	48.6 - 60.0	5
6.9 - 8.2	60.0 - 71.2	6
8.2 - 9.4	71.2 - 80.6	7

Table 7.1 : Optimum number of modulator elements when elements are lossy and total length is limited.

As a rule of thumb based on the above results, the modulator should be split so that the loss in the transmission-line of a single modulator element does not exceed 12 dB approximately.

Figure 2 illustrates how the normalized total phase contribution varies with α L,

with the number of modulation elements N as a parameter. For large values of α L the performance improves as $\sqrt{N}$ as long as N is much less than the optimum value.

8. Optimum Lengths - Velocity Mismatch Case

In the case of phase-velocity mismatch there is an optimum length for each modulating element. If the modulating element is made too long its phase contribution begins to decrease. If each modulating element is designed for this optimum length then the result derived in section 6 applies. However this is not quite the optimum use of the available power and length. The frequency response which results from phase-velocity mismatch will be discussed in section 9. It is:

$$R_N(1) = \frac{\sqrt{N}}{f} \sin\left(\frac{\pi f L (n_m - n_o)}{N c}\right) \qquad (20)$$

where

f is the frequency,
N is the number of modulating elements,
L is the total electrode length,
n_m and n_o are the modulating and optical refractive indices,
c is the velocity of light in free space.

The condition for the optimum number of modulator elements to be N is that

$$\frac{\sqrt{N-1}}{f} \sin\left(\frac{\pi f L (n_m - n_o)}{(N-1) c}\right) \leq \frac{\sqrt{N}}{f} \sin\left(\frac{\pi f L (n_m - n_o)}{N c}\right) \leq \frac{\sqrt{N+1}}{f} \sin\left(\frac{\pi f L (n_m - n_o)}{(N+1) c}\right) \qquad (21)$$

The optimum length for a single modulator element occurs when

$$\sin\left(\frac{\pi f L (n_m - n_o)}{c}\right) \text{ is a maximum} \qquad (22)$$

i.e. when

$$L = \frac{c}{2 f (n_m - n_o)} \qquad (23)$$

that is,

$$\frac{\pi f L (n_m - n_o)}{c} = \frac{\pi}{2} = 1.5708 \qquad (24)$$

This is obtained by using N=1 in expression (21). If we define a normalized length q,

$$q = \frac{\pi f L (n_m - n_o)}{c} \qquad (25)$$

then we can make up a table showing the values of q at which the optimal number of elements changes.

N Changes From → To	q	q/N(From)
1 → 2	1.57	1.57
2 → 3	2.83	1.41
3 → 4	4.0	1.33
4 → 5	5.20	1.30
5 → 6	6.35	1.27
10 → 11	12.23	1.22
100 → 101	118	1.18
1000 → 1001	1167	1.17

Table 8.1: Optimum Normalized Element Lengths for a Phase-Velocity-Mismatched Modulator.

Table 8.1 shows that when a large number of these modulator elements is used the optimum length for each one is a little less than that for a single element. As the modulator element approaches the single-element optimum length the last part of its length is making a very small contribution to the phase. This length would be used more efficiently in a new modulator element. For a given problem one can estimate a value of q from the above table and then assume that the modulator elements are effectively fixed by this. The theory of part 6, Length-Limited Modulator Elements, can then be used.

9. Frequency Response Effects - Velocity Mismatch Result

Previously we stated that there might be an optimum modulator element length. We gave the example of a modulator element with phase-velocity mismatch. However, in this case the optimum length only applies at a single frequency. The optimum length would decrease with increasing frequency. Consequently when the modulator is constructed from a number of shorter elements its frequency response changes. Figure 3

shows the frequency responses of four modulators, where the total power and interaction length are divided among N elements. The frequency response is proportional to

$$R_N(f) = \frac{\sqrt{N}}{f} \sin\left(\frac{\pi f L (n_m - n_o)}{N c}\right) \qquad (26)$$

where n_m, n_o are the modulation and optical refractive indices
c is the velocity of light

10. Frequency Effects - Loss Limited Result

The loss-limited result showed how to determine how many modulator elements to use when the attenuation over the length of the transmission-line was known. In general, however, the line attenuation is a function of frequency. Hence the result derived above is valid only at one particular frequency. Again, using a number of short modulator elements instead of a single, long modulator element changes the frequency response. Since attenuation generally rises with frequency, at low frequencies the number of modulator elements will be too big, so that better performance would have been obtained with fewer elements. At high frequencies the number of elements will be too small, so that better performance would be obtained with more elements. Of course as attenuation rises the performance gets worse no matter how many elements are used. As an example, let me assume that the attenuation varies as

$$\alpha = \alpha_o(1 + \sqrt{f/f_c}) \qquad (27)$$

and substitute this into expression (18) for total modulation. Figure 4 illustrates the result. As the number of modulation elements increases, the low-frequency responsivity decreases but the rolloff due to increasing attenuation at higher frequencies is slower.

11. Other Configurations

The above analyses by no means exhaust the possible configurations which could be used. For example the problem of phase-velocity mismatch can be addressed by using a number of short modulator elements which are fed in series instead of in parallel. For example, Alferness et al. [1] have demonstrated a phase-crossover structure which ensures that the phase error resulting from phase-velocity mismatch never exceeds 90°. A number of short modulator sections are connected together in series. Each section is

long enough to produce a 180° phase-drift of the modulation signal, and the sections are then connected together with crossovers to provide a 180° phase-correction between sections. This limits the phase error to ±90°. Schaffner [2] has demonstrated a related concept which also limits the maximum phase error at a center frequency. At the design center-frequency, an M-section modulator of this type acts like a single modulator element with no phase-velocity mismatch. As M increases, the length of this single modulator increases, and the limit on M occurs when the modulation signal attenuation over this length becomes severe. Thus, at the center frequency, a modulator of this type acts like a loss-limited modulator. Beyond a certain point, it may be better to use two such modulators, each with M/2 sections, instead of the single modulator with M sections. The limits on what is possible tend to depend on the details of the splitting and phasing of the modulation signal, factors which are not considered here.

The frequency response of a periodic phase-correcting modulator element is not the same as that of a simple modulator element. As the number of sections, M, increases, the bandwidth of the element about the design center-frequency decreases. This is because the phase-correction is frequency-dependent, so that phase errors reduce the sensitivity at other frequencies. In Figure 5 the effect of increasing M on the bandwidth of a modulator element of this type is shown.

12. Conclusion

Traveling-wave modulators suffer from phase-velocity mismatch and transmission-line attenuation. Where high modulation sensitivity is required at a specific frequency, it may be optimal to split the modulator into a number of shorter elements, each driven with a fraction of the available modulation signal power. We have shown how to determine the optimum configuration in the case of a modulator which suffers from neither problem, in the case of a modulator whose element lengths are fixed by some constraint, in the case of a lossy modulator and in the case of a phase-velocity-mismatched modulator. In addition we have examined the bandwidth implications of the various approaches.

References

[1] R.C. Alferness, S.K. Korotky, and E.A.J. Marcatili, "Velocity-Matching Techniques for Integrated Optic Traveling Wave Switch/Modulators," IEEE J. Quant. Electron., Vol. QE-20, pp 301 - 309, March 1984

[2] J.H. Schaffner, "Analysis of a Millimeter Wave Integrated Electro-Optic Modulator with a Periodic Electrode," Paper 13 at SPIE OE-LASE Conference 1217, Proceedings, pp. 101-110, Los Angeles, Calif., January 16-17, 1990

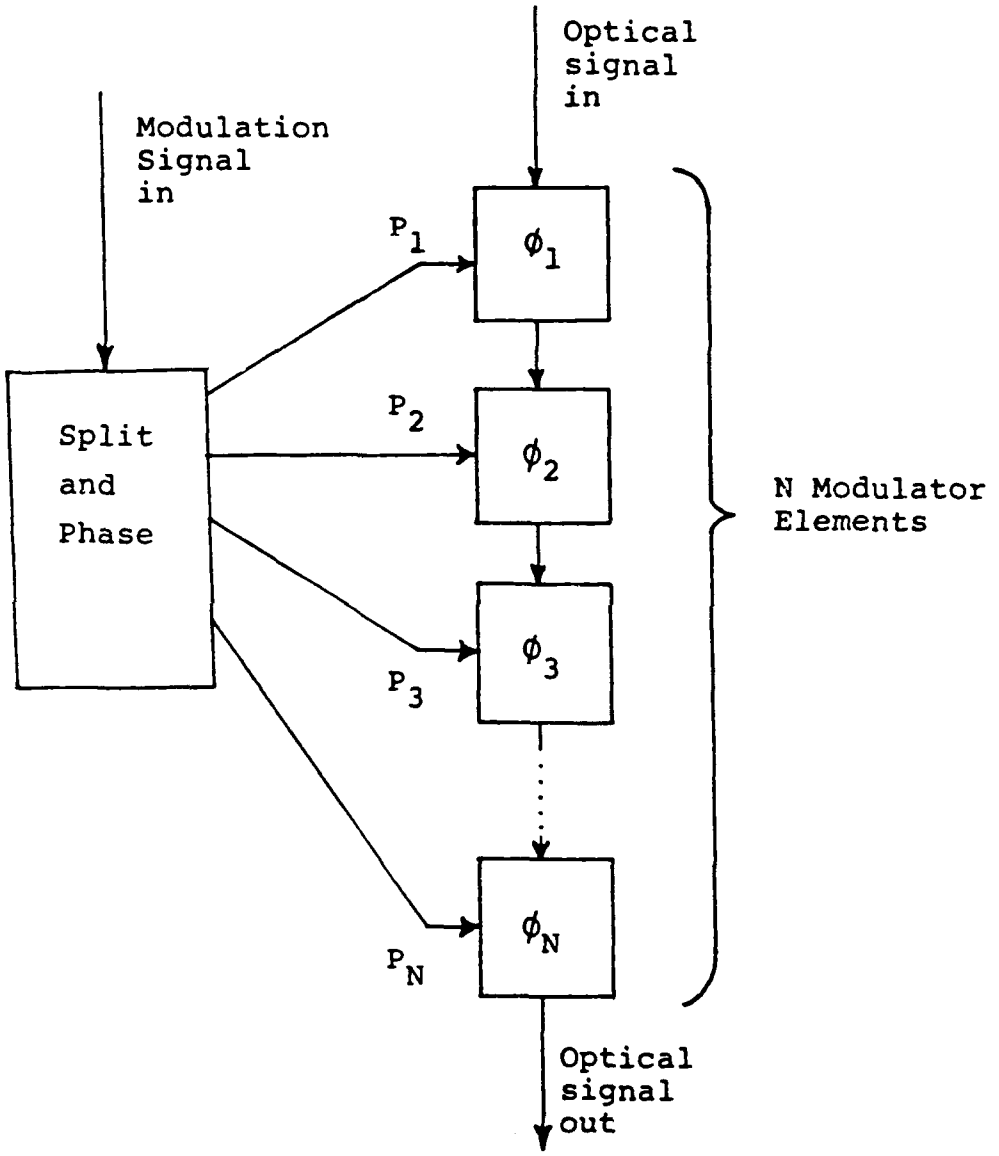

Figure 1: Modulator consisting of a number of modulator elements.

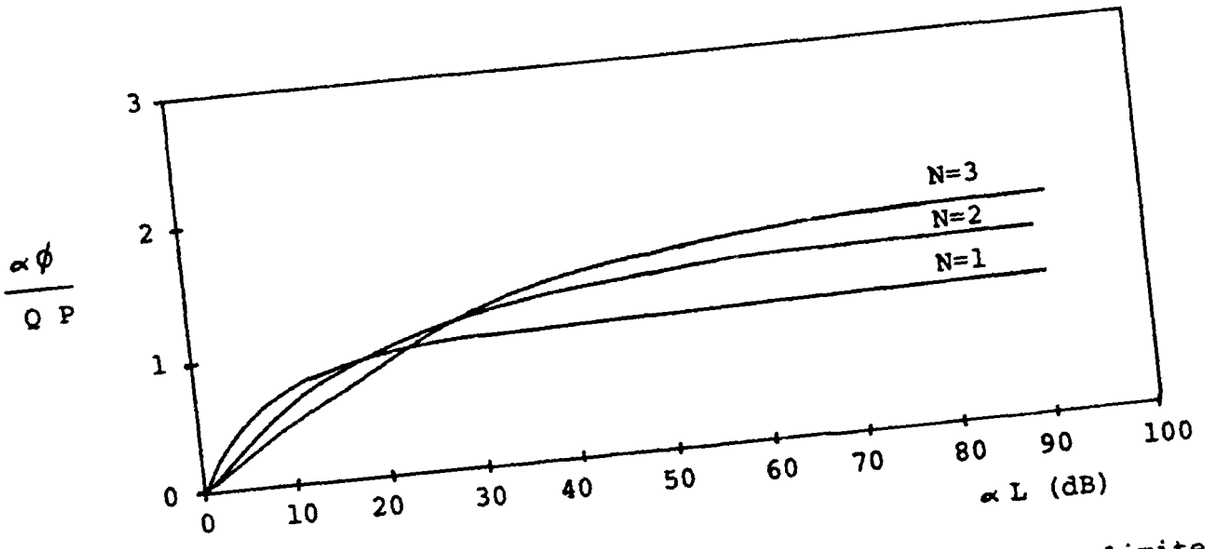

Figure 2: Performance of loss-limited modulators with 1,2, or 3 elements, as a function of attenuation.

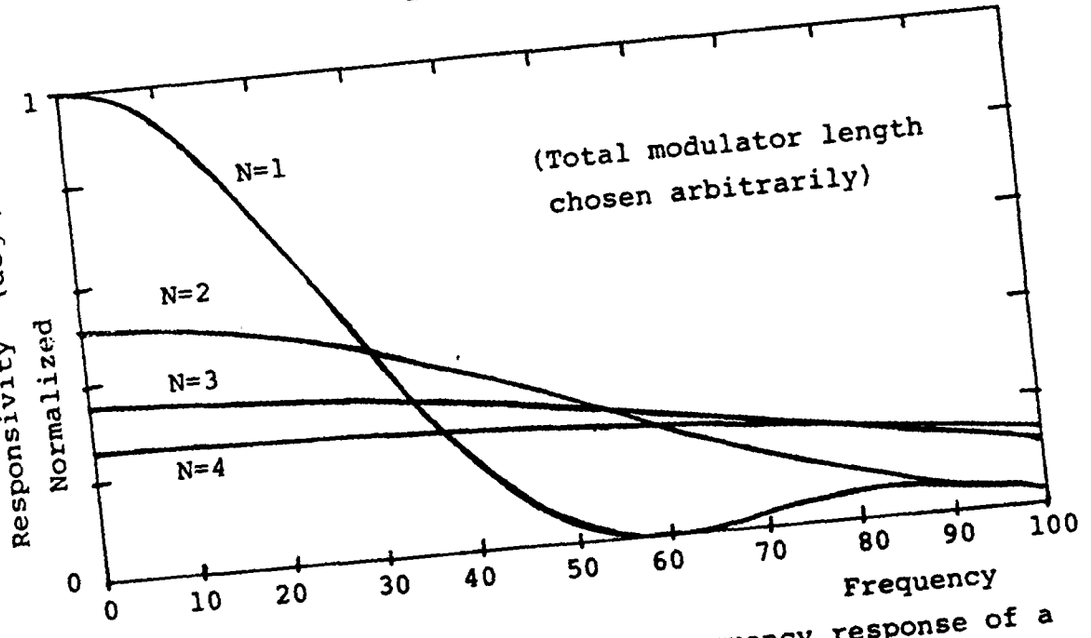

Figure 3: Frequency response of a modulator with phase-velocity mismatch when the length is split between 1,2,3, or 4 elements.

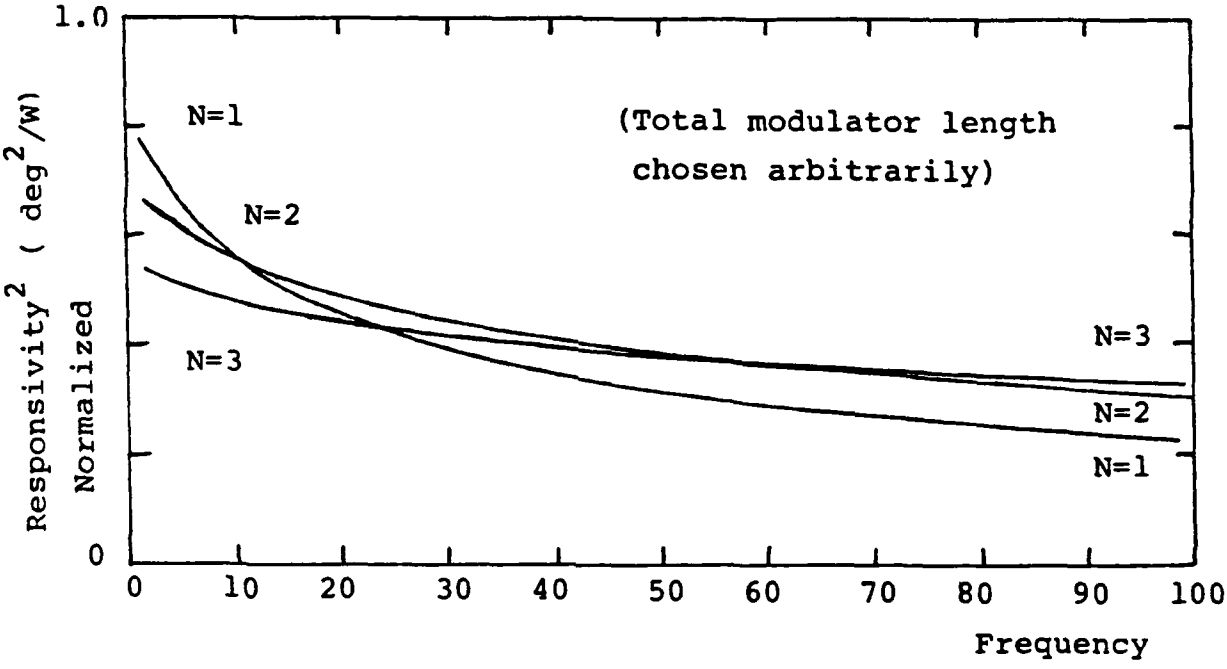

Figure 4: Frequency response of a loss-limited modulator when the total length is used as a single element, or broken into 2 or 3 elements.

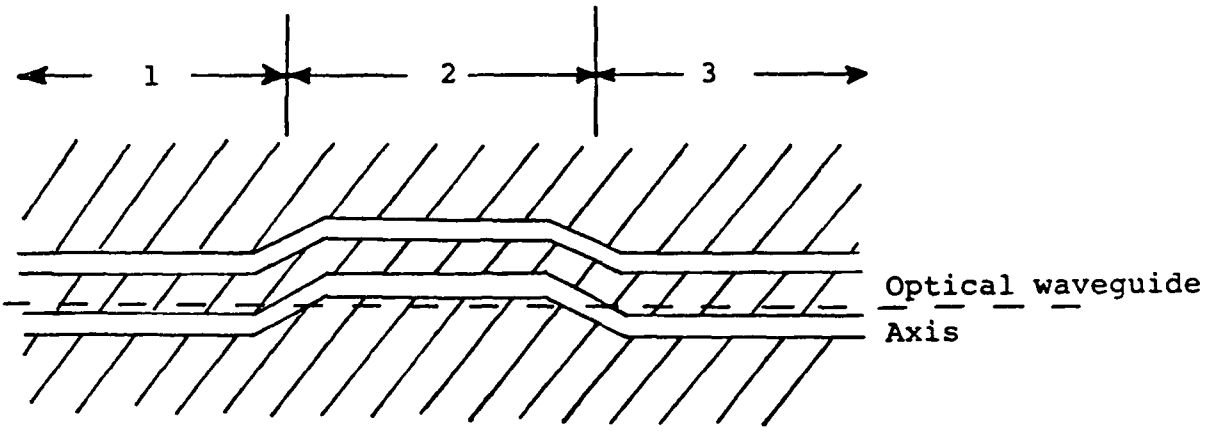

M=3 phase-reversal-type modulator element

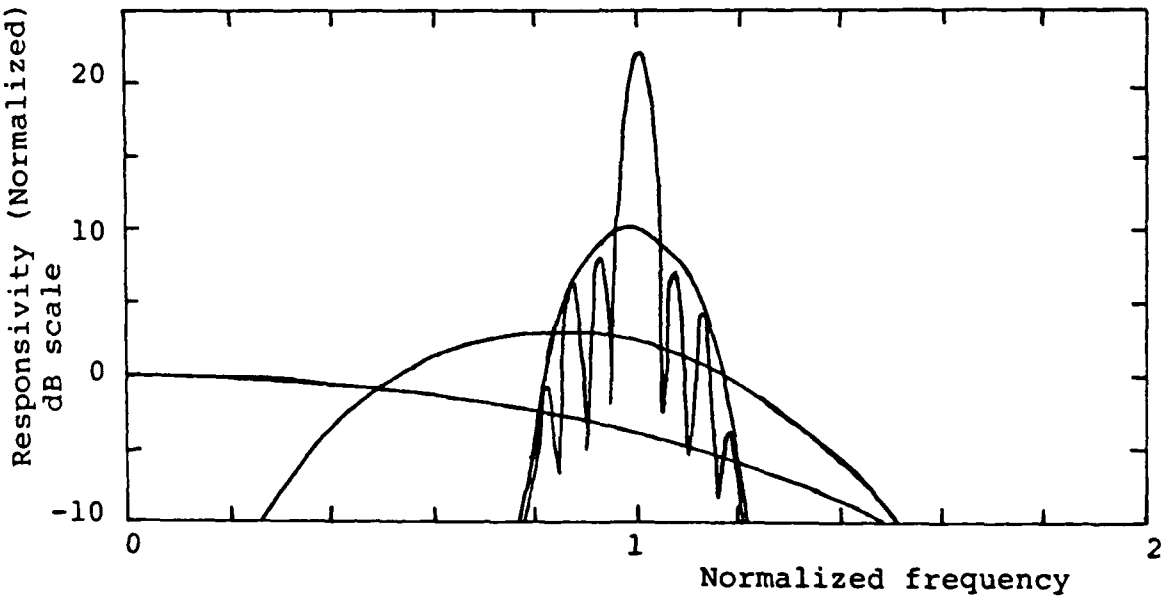

Figure 5: Phase-reversal-type modulator and frequency response for 1,2,5, and 20 sections.

Index

Glossary

Antenna pattern: Any antenna will radiate power more in some direction(s) than in others. The quantitative description of the way in which a particular antenna distributes the power it radiates is the antenna pattern.

Band designations:

X-band: The frequency range 8.2 - 12.4 GHz
K-band: The frequency range 18 - 26.5 GHz
V-band: The frequency range 50 - 75 GHz
W-band: The frequency range 75 - 110 GHz

Dispersion: The dependence of signal propagation velocity on signal frequency (or, equivalently, on signal wavelength). May be due to the material in which the signal is propagating, or may be due to the structure of the waveguide.

Electro-optic effect: A property of some materials, where the refractive index of the material is a function of the electric field strength. This means that the velocity of an optical signal through the material can be controlled by an electric field.

Fabry-Perot interferometer: An optical filter with a very narrow passband. In this report the filter passband is swept (scanning Fabry-Perot) so that the interferometer is used as an optical spectrum analyser.

H-plane antenna pattern: The antenna pattern in the plane (of symmetry) where the magnetic fields (H) lie in the plane and the electric fields (E) are everywhere normal to it.

$LiNbO_3$: Lithium Niobate; a transparent crystalline material which displays a strong electro-optic effect.

Mach-Zehnder amplitude modulator: Amplitude modulator produced by splitting the input optical beam into two paths, phase-modulating the paths separately, then recombining the paths into one beam. If the phase-difference between the paths is zero, the output intensity will be a maximum. If the phase-difference is 180°, the output intensity will be zero (or a minimum).

mm-wave: Millimeter-wave; the frequency range 30 - 300 GHz. Often the word "microwave" is intended to include all or part of the millimeter-wave range.

Phase velocity: The velocity at which any phasefront of the wave (e.g. the point at which the electric field is zero) propagates in the direction of interest.

Refractive index: The ratio of the speed of light in a vacuum to the speed of the signal in the material.

Terminated (transmission-line): A transmission-line which is connected to a load. Usually this implies that the load impedance is equal to the characteristic impedance of the transmission-line, so that no power is reflected back into the transmission-line by the load.

Sensitivity: In this report, sensitivity refers to the optical phase-deviation produced by 1 Watt of mm-wave (RF) power. Units are degrees/$\sqrt{\text{Watt}}$.

WR-15: A standard rectangular metal waveguide with internal dimensions 0.075 x 0.15 inches. Its cutoff frequency is 39.9 GHz. It is usually used in the frequency range 50 - 75 GHz (V-band).

WR-137: A standard rectangular metal waveguide with internal dimensions 0.685 x 1.37 inches. Its cutoff frequency is 4.3 GHz. It is usually used in the frequency range 5.46 - 8.20 GHz.

ϵ (sometimes ϵ_r): Relative dielectric constant. If the absolute dielectric constant of the material is designated ϵ_m, then

$$\epsilon = \frac{\epsilon_m}{\epsilon_o}$$

where $\epsilon_o = 8.854 \times 10^{-12}$. ϵ is dimensionless, and its magnitude is greater than or equal to 1. Since absolute dielectric constants have magnitudes less than 10^{-8}, there can be no ambiguity between ϵ and ϵ_m.

*U.S. GOVERNMENT PRINTING OFFICE

MISSION

OF

ROME LABORATORY

Rome Laboratory plans and executes an interdisciplinary program in research, development, test, and technology transition in support of Air Force Command, Control, Communications and Intelligence (C^3I) activities for all Air Force platforms. It also executes selected acquisition programs in several areas of expertise. Technical and engineering support within areas of competence is provided to ESD Program Offices (POs) and other ESD elements to perform effective acquisition of C^3I systems. In addition, Rome Laboratory's technology supports other AFSC Product Divisions, the Air Force user community, and other DOD and non-DOD agencies. Rome Laboratory maintains technical competence and research programs in areas including, but not limited to, communications, command and control, battle management, intelligence information processing, computational sciences and software producibility, wide area surveillance/sensors, signal processing, solid state sciences, photonics, electromagnetic technology, superconductivity, and electronic reliability/maintainability and testability.